Biogeosciences Discuss., 9, 18211–18252, 2012
www.biogeosciences-discuss.net/9/18211/2012/
doi:10.5194/bgd-9-18211-2012

Biogeosciences
Discussions

Sediment transport along the Cap de Creus Canyon flank during a mild, wet winter

J. Martín[1], X. Durrieu de Madron[2], P. Puig[1], F. Bourrin[2], A. Palanques[1], L. Houpert[2], M. Higueras[2], A. Sanchez-Vidal[3], A. M. Calafat[3], M. Canals[3], and S. Heussner[2]

[1]Institut de Ciències del Mar (CSIC), Passeig Marítim de la Barceloneta 37–49, 08003, Barcelona, Spain
[2]CEFREM, CNRS-Université de Perpignan, Via Domitia, 52 avenue Paul Alduy, 66860, Perpignan, France
[3]GRC Geociències Marines, Departament d'Estratigrafia, Paleontologia i Geociències Marines, Facultat de Geologia, Universitat de Barcelona, Campus de Pedralbes, Martí i Franquès s/n, 08028 Barcelona, Spain

Received: 28 November 2012 – Accepted: 30 November 2012 – Published: 14 December 2012

Correspondence to: J. Martín (jmartin@icm.csic.es)

Published by Copernicus Publications on behalf of the European Geosciences Union.

Abstract

Cap de Creus Canyon (CCC) is known as a preferential conduit for particulate matter leaving the Gulf of Lion continental shelf towards the slope and the deep basin, particularly in winter when storms and dense shelf water cascading coalesce to enhance the seaward export of shelf waters.

During the CASCADE (CAscading, Storm, Convection, Advection and Downwelling Events) cruise in March 2011, deployments of recording instruments within the canyon and vertical profiling of the water column properties were conducted to study with high spatial-temporal resolution the impact of such processes on particulate matter fluxes.

In the context of a mild and wet 2010–2011 winter, no remarkable dense shelf water formation was observed. On the other hand, the experimental setup allowed to study the impact of E-SE storms on the hydrographical structure and the particulate matter fluxes in the CCC. The most remarkable feature in terms of sediment transport was a period of dominant E-SE winds from 12 to 16 March, including two moderate storms of significant wave heights = 4–4.5 m. During this period, a plume of freshened, relatively cold and turbid water flowed at high speeds along the southern flank of CCC in an approximate depth range of 150–350 m. The density of this water mass only reached $\sim 28.78\,\mathrm{kg\,m^{-3}}$, indicating that it did not cascade into the canyon and that merely downwelled into it forced by the accumulation of seawater along the coast during the storms and by the subsequent strong cyclonic circulation induced over the shelf. Suspended sediment load in this turbid intrusion was comparable at three heights above bottom where turbidimeters were installed (10, 75 and 115 m above bottom) on the southern canyon flank and oscillated between 10 and 50 $\mathrm{mg\,L^{-1}}$. Current speeds were also comparable in the depth range profiled by ADCPs (40 to 150 mab) and reached values up to 90 $\mathrm{cm\,s^{-1}}$ during the peak of the strongest storm (13 March, $H_s = 4.5$ m).

Sediment transport at 75 mab on the southern canyon flank was estimated at 1–1.5 $\mathrm{t\,m^{-2}}$ for the entire deployment while very close to the bottom (5 m above) in the canyon head it was less than 0.6 $\mathrm{t\,m^{-2}}$ during the same period. We provide a rough

estimation of 10^5 t of sediment transported through the canyon along its southern wall during a 3 day-long period of storm-induced downwelling.

Following the veering of the wind direction (from SE to NW) on 16 March, downwelling ceased, currents inside the canyon reversed from down to up-canyon, and the turbid shelf plume was evacuated from the canyon, most probably flowing along the southern canyon flank and being entrained by the general SW circulation after leaving the canyon confinement.

This study highlights that remarkable sediment transport occurs in the CCC, and particularly along its southern flank, even during mild and wet winters, in absence of cascading and under limited external forcing. The sediment transport associated to eastern storms like the ones described in this paper tends to enter the canyon by its downstream flank, partially affecting the canyon head region. Sediment transport during these events is not constrained near the seafloor but distributed in a depth range of 200–300 m above the bottom. Our paper broadens the understanding of the complex set of atmosphere-driven sediment transport processes acting in this highly dynamic area of the northwestern Mediterranean Sea.

1 Introduction

Continental margins are transitional areas between the land masses and the open sea where inputs of particulate matter from the former tend to accumulate due to gravitational settling of river plumes and the physical barrier imposed by along-shore currents and density fronts. Under certain conditions, sediments previously stored on the coast and the continental shelf can be remobilized and transported to greater depths. This transfer of organic and inorganic matter from shallow depths to the continental slope and the deep basins strongly influences biogeochemical cycles, the structure and functioning of benthic ecosystems and the fate of pollutants delivered from coastal point sources (Jahnke et al., 1990; Pfannkuche, 1993; Puig et al., 1999).

Some processes that contribute to facilitate the across-isobath exchange of water masses and entrained particulate matter are instabilities and meandering of slope currents (Flexas et al., 2002), wind-induced downwelling and upwelling or the development of buoyancy-driven currents flowing downslope (Huthnance, 1995). Also, the presence of submarine canyons intersecting continental shelves can enhance across-shelf sediment transport, by intercepting the along-shore sediment drift, promoting and intensifying ageostrophic flows, focusing internal waves and tides or channelling density currents (Hickey, 1997; Puig et al., 2004; Martín et al., 2007, 2011; Allen and Durrieu de Madron, 2009; Palanques et al., 2011).

During the last decades, the Gulf of Lion (GoL) in the northwestern Mediterranean has been targeted by numerous observational programs covering different aspects of its present-day particle flux dynamics (Monaco et al., 1990; Heussner et al., 1996, 2006; Durrieu de Madron et al., 2008). Its wide continental shelf indented by numerous submarine canyons, the significant freshwater inputs feeding the shelf with terrestrial sediments, an energetic oceanographic and meteorological regime combined with very weak tidal motions, has made of the GoL a natural laboratory to study land-to-basin sediment transport processes driven mainly by sea-atmosphere interactions.

The Cap de Creus Canyon (CCC) at the western end of the GoL is widely acknowledged as the main route for particulate matter transfer from the GoL coast and continental shelf to the slope and deep basin (Canals et al., 2006; Palanques et al., 2006; De Geest et al., 2008). Most of the published literature on the off-shelf delivery of sediments through the CCC has focused on the impact of extreme events such as major floods and storms (Guillén et al., 2006; Bourrin et al., 2008), deep cascading (Canals et al., 2006; Puig et al., 2008; Palanques et al., 2012) or the combination of them (Palanques et al., 2006; Ulses et al., 2008a).

The CASCADE (CAscading, Storm, Convection, Advection and Downwelling Events) cruise (1–23 March 2011) was designed to study with high resolution the main processes of water and mass transport operating from the shelf to the deep basin in the GoL region. A main task of the experimental design was to quantify the fluxes of organic and inorganic matter associated to open sea convection, dense shelf water cascading and storms impinging on the continental shelf.

This work makes use of hydrographical, hydrodynamic and particle flux data collected during CASCADE to study with unprecedented spatial and temporal resolution the effects of dense shelf water cascading and/or eastern storms in shelf-slope exchanges of water and particulate matter through the Cap de Creus submarine canyon.

2 Study area

The GoL is a micro-tidal, river-dominated continental margin stretching along a substantial part of the French Mediterranean, from Cap Croisette in the northeast to Cap de Creus in the southwest. The continental shelf is wide and indented by submarine canyons mainly on its distal part. River discharge in the GoL is largely dominated by the Rhône River, the largest freshwater source opening to the western Mediterranean and likewise the main sediment source feeding the GoL. Additionally, numerous smaller rivers can yield significant inputs of freshwater and particulate matter in the form of flash floods (Bourrin et al., 2006). Most of the sediments delivered by GoL rivers are temporarily stored near their mouths (Drexler and Nittrouer, 2008) and afterwards remobilized and redistributed along the shelf by the action of storms and along-shore currents (Guillén et al., 2006).

The GoL is subject to an energetic meteorological regime, mainly during winter. On one hand, north (Tramontane) and northwest (Mistral) cold and dry winds induce loss of buoyancy of surface shelf waters through cooling and evaporation, eventually leading to the downslope sinking of surface waters until they reach their compensation depth, sometimes involving overspill from the shelf towards the slope in a phenomenon known as Dense Shelf Water Cascading (DSWC) (Bougis and Ruivo, 1954; Durrieu de Madron et al., 2005). On the other hand, SE-E ("Marin") winds produce larger swells and significant erosion on the shelf (Guillén et al., 2006). The interplay of DSWC and shelf storms has been recognised as the main mechanism fuelling the offshore redistribution of particulate matter from the GoL (Durrieu de Madron et al., 2008; Palanques et al., 2008).

The across-margin export of total and organic matter in the GoL takes place preferentially through a network of submarine canyons (Buscail and Germain, 1997), which is one of the densest of the World Ocean (Harris and Whiteway, 2011). Nonetheless, the capacity to foster off-shelf sediment transport is not evenly distributed among GoL canyons, but tends to increase from east to west (Monaco et al., 1990; Heussner et al., 1996, 2006; Palanques et al., 2006). This longitudinal gradient is a result of the morphology of the margin (the distance from canyon heads to the coast decreases westward) and also of the hydrodynamic regime over the GoL, which is primarily governed by an along-slope current flowing cyclonically as part of the Northern Current, a larger oceanographic feature that extends from the Gulf of Genoa to the Gulf of Valencia (Millot, 1999). Coupled to the along-slope current, a density front is established between freshened shelf waters and denser open-sea water, which further reinforces the along-shore confinement of shelf waters and river plumes. The general westwards circulation promotes a convergence of water and entrained particles at the southwestern end of the GoL, a trend that is greatly enhanced under E-SE winds, which enhance the cyclonic circulation on the GoL shelf and produces a sea level rise next to the coast, altogether promoting downwelling conditions (Ulses et al., 2008b; Palanques et al., 2008). Suspended sediments are also effectively pulled towards the southwestern end of the Gulf during these events, owing to the entrainment of river plumes and mainly to the resuspension and advection of previously settled particles, given that erosion of shelf sediments is maximal under E-SE storms (Ferré et al., 2005; Guillén et al., 2006).

At the very end of the western GoL, the continental shelf narrows rapidly and the Cap de Creus peninsula (Fig. 1) imposes a barrier to the flow, exacerbating the concentration of water and entrained particles. Next to this geomorphologic bottleneck lies the Cap de Creus Canyon (CCC), deeply carved across the continental slope and thus offering a preferential route for water flowing along the shelf at depths below the canyon rim. Previous studies have ascertained that the CCC constitutes the main route for particulate matter dispersal from the GoL to the slope and deep basin, in particular during intense meteorological events when sediment fluxes can be up to two orders of magnitude higher in the CCC than in any other GoL canyon (Canals et al., 2006; Palanques et al., 2006, 2012).

Shelf-to-basin transport is maximal during winters of intense DSWC, as it was the case during 1998–1999, 2004–2005 and 2005–2006 (Heussner et al., 2006; Canals et al., 2006; Palanques et al., 2012). Together with the off-shelf transport of dissolved and particulate matter entrained in the sinking dense water masses, the high water currents during these episodes have the potential to erode and shape the deep canyon floor (Canals et al., 2006; Puig et al., 2008).

Hydrology in the northwestern Mediterranean and particularly in the GoL is complex and very variable, with the presence of various water masses that result from a wide range of mixing between exogenous water types, water masses formed locally or in adjacent areas, and freshwater inputs. The external water types are the Atlantic Water (AW) and the Levantine Intermediate Water (LIW). The AW fills the upper ∼250 m of the western Mediterranean and has its origin in the inflow of Atlantic waters at the Gibraltar Strait. After being severely modified during its long transit towards the study area, the characteristics of the so-called "old" Atlantic Water (oAW) at the GoL are $T = 15$–$17\,^{\circ}$C and $S = 36.25$–36.50 (Salat and Cruzado, 1981). The salty and warm LIW originates in the eastern Mediterranean and enters the western basin through the Strait of Sicily as an intermediate water mass infilling approximately the 250–800 m depth strata of the NW Mediterranean water column. The hydrological characteristics of LIW at the study area are variable depending on its age and hence its degree of mixing with other water masses but nonetheless display a clear salinity maximum ($S > 38.45$) and relative temperature maximum ($T > 13\,^{\circ}$C) in hydrological profiles. During winter, strong, cold and dry northerlies promote the formation of Dense Shelf Waters over the GoL ($T < 13\,^{\circ}$C; $S < 38.4$) (Dufau-Julliand et al., 2004; Durrieu de Madron et al., 2005). Depending on the strength of winter cooling and evaporation and also on the degree of stratification of the water column, dense shelf waters can reach the deep basin and thus contribute to modify the deep Northwestern Mediterranean Water, or they can detach at intermediate according to their buoyancy compensation level. In this latter case, Western Intermediate Waters (WIW) are formed, with characteristics $T = 12.6–13.0\,^{\circ}\mathrm{C}$; $S = 38.10–38.30$ (Lapouyade and Durrieu de Madron, 2001).

3 Materials and methods

3.1 Instrumented mooring lines

3.1.1 Temporary lines

Two instrumented mooring lines were deployed during the CASCADE cruise along the western flank of the CCC at 42°21.61′ N, 3°20.42′ E (SF1, water depth = 290 m) and 42°20.31′ N, 3°23.23′ E (SF2, water depth = 365 m), respectively. The relative positions of these mooring sites within the canyon are displayed in Fig. 1b. The mooring lines were deployed on 3 March and recovered on 21 March 2011.

Both lines were equipped with a similar array of instruments, comprising a downward-looking 300 kHz Teledyne RDI Acoustic Doppler Current Profiler (ADCP) at 160 m above the bottom (mab), three Seapoint turbidimeters (AQUA logger 520 from Aquatec Group) at 10, 75 and 115 mab respectively, a Technicap PPS3/3 sediment trap at 40 mab and a Seabird SBE 37-SMP probe at 8 mab. ADCPs profiled 110 m of water column (from 40 to 150 mab) in 2 m-wide cells at a sampling rate of 5 min. The SBE37SMP probe measured temperature, conductivity and pressure every 3 min. Depth, potential temperature, practical salinity and potential density anomaly were calculated based on the equation of state of seawater EOS-80 (Fofonoff and Millard, 1983). Seapoint turbidimeters were programmed to measure water turbidity in Formazin Turbidity Units (FTU) every 20 s in auto-gain mode. FTU values were transformed into suspended sediment concentration (SSC, mg L^{-1}) using the calibration by Guillén et al. (2000).

Current data was rotated when necessary to meet the main canyon axis direction (~ 130°). Reported positive (negative) values are considered up-canyon (down-canyon). To calculate sediment transport, data from turbidimeters and the corresponding ADCP cells/punctual current-meters at similar depths were combined to obtain the sediment flux in units of $g\,m^{-2}\,s^{-1}$. This approach could be applied only to the two depths in SF1 and SF2 (75 and 115 mab) and near-bottom (5 mab) at CH, where simultaneous turbidity and current measurements were available.

Sediment traps were programmed to sample the downward particle flux at 35 h intervals. In order to avoid grazing by zooplankton and the remineralization of organic compounds, the cups were poisoned with 2 % formaldehyde in filtered seawater prior to deployment. The procedures used to treat sediment trap samples and to obtain the downward fluxes ($g\,m^{-2}\,d^{-1}$) are described in Heussner et al. (1990). Grain size analysis of trap samples was performed on a Coulter LS 230 Laser Particle Size Analyzer, after pre-treatment of the dry sample with 10 % H_2O_2 and sodium polyphosphate solution to remove organic matter and disaggregate the sample.

3.1.2 Long-term mooring line at the canyon head

In addition to the two high-resolution, short-lived mooring deployments, an additional mooring line was present at the CCC head (42°23.15′ N, 3°19.53′ E; 300 m depth; Fig. 1), as part of a long-term monitoring program active since autumn 2004. This line was equipped with a near-bottom set of instruments comprising an Aanderaa RCM9 current meter (5 mab; sampling rate 30 min), an AQUA logger 520 Seapoint turbidimeter (6 mab; sampling rate 2 min) and a Technicap PPS3/3 sediment trap (25 mab; sampling interval 15 days). Data from this line will be used to weigh the relevance of water and particle fluxes along the southern canyon flank against those on the canyon head, and also as a reference to put the main study period (3–21 March 2011) into a broader perspective.

3.1.3 Data quality check

The dynamics of the mooring lines were assessed using the Mooring Design and Dynamics (MDD) software (Dewey, 1999) and validated by comparing the modelled deepening of the line to the pressure sensor located in the ADCP units. The simulation of the behaviour of the ADCP at 160 mab and the sediment trap at 40 mab for different observed speeds compared well with the observed deepening of the line (Fig. 2). Deepening and tilting increased markedly under current speeds surpassing 40 cm s^{-1} (an approximate 30 % of current records were above that threshold at both lines). According to the MDD simulations, during the maximum current speeds (90 cm s^{-1}) recorded during this study, the sediment traps originally at 40 mab deepened to only a few meters above the seafloor and its inclination was nearly horizontal. Such high velocities were rarely reached. At line SF2 currents were higher than 80 cm s^{-1} only 0.4 % of the time, while at SF1 the highest speed range (70–80 cm s^{-1}) was reached 0.3 % of the recording time. These results raise concerns particularly over the validity of sediment trap-derived particle fluxes during high current speed periods, which will be considered hereafter as qualitative data. On the other hand, the remarkable homogeneity of currents estimated at the two critical (due to the concomitant presence of turbidimeters at the same points) ADCP bins during the episodes of maximum current speed (Fig. 2), indicates that ADCP deepening has not severely affected the reliability of these ADCP bins and they can be ascribed to its nominal depths (75 and 115 mab) in spite of the transitory depth changes.

3.2 Hydrological vertical profiling and ship-based ADCP data

Vertical profiling of water column properties was conducted intensively during the CASCADE cruise, covering a wide set of coastal, shelf, slope and open sea stations. The CTD profiles used in this work are restricted to the Cap de Creus Canyon area and comprise a high resolution temporal sampling at a single station between the two temporary mooring lines, and two cross-canyon transects (see Fig. 1b for station locations).

The CTD probe used was a Seabird 911Plus. Pressure, water temperature, conductivity and turbidity, among other parameters, were recorded at a rate of 24 Hz, from the surface to a few meters above the seafloor whenever possible. A low-pass filter was used to compensate for the different time response of the sensors and to remove outliers. A ship-roll and minimum probe velocity filter ($<0.10\,\mathrm{m\,s^{-1}}$) was applied to each cast to disallow pressure slowdowns and reversals. After filtering, the downcast portion of each cast was pressure-averaged and sequenced into 1 db pressure intervals. The 1 db-averaged pressure, temperature and conductivity data were used to compute depth, potential temperature, salinity and potential density anomaly. Temperature is ITS-90 and salinity is PSS-78. Density was calculated based on the equation of state of seawater EOS80 (Fofonoff and Millard, 1983). Water turbidity, measured in FTU units by a Seapoint sensor, was transformed into suspended sediment concentration (SSC) following the calibration by Guillén et al. (2000). Current speed data from a ship-based ADCP (RDI-Ocean Surveyor, 38 kHz) profiling 0–700 m at 16-m wide cells have also been used. The ADCP data were processed with the Common Oceanographic Data Access System (CODAS) software (Firing et al., 1995), in agreement with the best practices suggested by the Go-Ship Group (Firing et al., 2010). Bottom-track calibration was made to determine precisely transducer orientation relative to the heading sensor and then the data were corrected for possible problems in the navigation recordings and bad ADCP bins/profiles.

3.3 Meteorological, wave and river discharge data

Water discharge of rivers opening to the Gulf of Lion was measured by gauging stations located near river mouths and provided by the Compagnie Nationale du Rhône and the Banque HYDRO (French Ministry of Environment). Significant wave height, peak period and wave direction from north were calculated from wave measurements obtained by means of an upward-looking 600 kHz Teledyne RDI ADCP equipped with a wave gauge, deployed at 27 m depth as part of the POEM coastal monitoring site (see

Fig. 1a for location). A meteorological buoy installed at the same site provided wind speed and direction.

4 Results

4.1 General setting for winter 2010–2011

Time-series of meteorological and wave data recorded by the POEM buoy at the Têt river mouth and water discharge of rivers opening to the Gulf of Lion during winter 2010–2011 are shown in Fig. 3. In order to understand the sediment fluxes observed during the CASCADE cruise in a broader context, near-bottom temperature, suspended sediment concentration (SSC) and downward mass flux at the permanent monitoring station in the canyon head (CH, see location in Fig. 1b) during the entire winter 2010–2011 are also shown in Fig. 3.

As usual in the study area during wintertime, the most frequent and in general stronger winds were NW (Tramontane), alternated by shorter periods of E-SE (Marin) winds and others periods more variable. A period of sustained Tramontane with wind speeds up to 12 $\mathrm{m\,s^{-1}}$ preceded the beginning of the CASCADE cruise (1–23 March 2011). During the cruise itself, eastern winds and storms attained the highest frequency of all the winter and were particularly persistent and intense from 12 to 16 March. Three E-SE storms hit the GoL shelf during the study, peaking on 8, 13 and 15 March with significant wave heights 3.3, 4.6 and 4.1 m respectively. In all three cases wave peak period was between 9 and 10 s. These values correspond to average winter storms in the region. The 13 March storm was the most remarkable of the three in terms of coastal erosion, particularly in the central GoL, although its effects were comparatively milder in the western sector of the Gulf (DREAL, 2011).

The sustained E and SE winds from 12 to 16 March pulled a Mediterranean humid air mass towards southern France, forcing precipitation by orographic control on the Massif Central and mainly the Pyrenees. In contrast, precipitations where abnormally weak in the rest of France including most of the Rhône watershed (http://www.eaufrance.fr/docs/bsh/2011/04/precipitations.php). As a consequence, the contribution of regional rivers to the total water discharge in the GoL was unusually high, accounting for up to 70 %, contrasting with a usual contribution of only 10–20 % (the rest corresponding to the Rhône River alone). The strongest river discharges coincided with the change of wind direction from E-SE to NW around 16 March.

Several decreases of near-bottom temperature simultaneous to increases of current speed were observed at the canyon head, in general associated to E-SE storms or strong Tramontane wind gusts. It is also noteworthy that horizontal and especially downward particle fluxes at the canyon head were even lower during the period of eastern storms and river flooding in March than early in the winter, particularly in December when water temperature decreases were strongest (Fig. 3). Hence, from the perspective of the canyon head, which has been often used as a reference for the activity of the CCC, we are dealing with a weak winter in terms of sediment transport, and this is particularly applicable to the main study period (March 2011).

4.2 Currents and sediment fluxes at the canyon head during the CASCADE cruise

Water temperature, current speed and particle flux data at the canyon head station from 1 to 23 March 2011 along with basic hydro-meteorological parameters obtained during the same period are shown in detail in Fig. 4.

Following a 10-day long period of NW winds just before the beginning of the cruise, near-bottom currents were directed down-canyon simultaneously to a decrease of near-bottom water temperature from 3 to 6 March. This trend reversed back by 7 March, when currents were weaker, up-canyon and temperature was higher than 13 °C, suggesting the presence of LIW at the canyon head. On 8 March, the first eastern storm ($H_s = 3.3$ m) of the monitored period hit the western GoL. For the two days following this storm, currents (up to 45 cm s^{-1}) were directed downcanyon and LIW withdrew from the canyon head. This storm did not cause a noticeable increase at the monitored station in terms of horizontal or downward mass fluxes. On the contrary, the two combined eastern storms of 12 and 15 March left a clear imprint in the canyon head, in terms both of current speed ($>60\,\mathrm{cm\,s^{-1}}$) and SSC, resulting in downcanyon horizontal fluxes of suspended sediments between 3 and $4\,\mathrm{g\,m^{-2}\,s^{-1}}$. The sum of regional rivers discharge peaked between 16 and 17 March, that is, after the main period of downcanyon particle flux. After 16 March, severe fouling of the acoustic sensor prevented the estimation of SSC. In any case, the transport associated to a hypothetical increase of SSC after 17 March would have not been significant taking into account the low current speeds from that date till the end of the cruise (Fig. 4). Cumulative sediment transport at 5 mab at the canyon head was slightly lower than $0.6\,\mathrm{t\,m^{-2}}$ for the entire study period.

4.3 Sequence of hydrological changes in the water column during the 12–14 March stormy period

On 11 March, in coincidence with the approach of the strongest eastern storm of the 2010–2011 winter, R/V *l'Atalante* positioned on a fixed station (CX) in the CCC to monitor the effects of the storm on the hydrology and particle fluxes in the canyon with high temporal resolution. The location of CX was chosen in an intermediate position between the 2 temporary moored lines (nominal position: 42°20.70′ N; 3°21.64′ E, 292 m depth; see Fig. 1b). 32 consecutive CTD casts were conducted at this station from 11 March at 21:45 to 14 March at 06:28 (UTC time).

Contour plots of water temperature, salinity, density and turbidity data during this period are plotted in Fig. 5. Water currents were also monitored by means of a ship-based ADCP. Current speed and direction at 210 m depth (the deepest ADCP cell that provided valid measurements) are also shown in Fig. 5.

During the first phase of monitoring at the CX station (11–12 March), warmer and less dense water was progressively pushed down, eventually reaching the seafloor at 300 m depth. An increase of turbidity is also noticed near the bottom on 12 March, likely related to the forced displacement of the resident water, as also indicated by increasing current speeds (Fig. 5). Worsening weather conditions on the night of 12–13 March caused an accident that forced to discontinue the CTD casts from 12 March at 23:06 to 13 March at 07:33. Once the CTD was fixed and vertical profiling resumed, the hydrological structure of the water column had drastically changed. A water mass characterized by relatively low salinity (37.65–38.00), low temperature (11.5–12.5 °C) and high oxygen content (5.5–5.7 mg L^{-1}) had occupied the deepest layer (~ 200–300 m depth) of the canyon at the CX station. Currents at 210 m depth also changed notably between the two sampling phases here considered, from relatively weak and isotropic currents at the beginning of the measuring period to much stronger (up to 90 cm s^{-1}) and clearly oriented along-canyon (130°) when the cold water intrusion appeared near the bottom.

Two across-canyon CTD transects were conducted after the monitoring at the CX station was completed. The first one was conducted just immediately on 14 March, still under conditions forced by the prevalent easterlies. The second one was conducted on 21 March after a period of northerlies. The across-canyon contours of salinity, temperature, density anomaly, oxygen content and suspended sediment concentration for each of these transects are shown in Fig. 6.

The 14 March transect (Fig. 6a) reveals the same bottom water mass observed at station CX, flowing along the southern canyon in an approximate depth range 150–350 m and extending about 2 km from the flank into the canyon axis. SSC within the plume lies in the range 2–14 mg L^{-1}. Underlying this freshened, cold and turbid water mass, a water mass with the hydrological characteristics of WIW could be detected. Further deeper into the canyon axis, LIW was apparent at ~ 500 m depth.

A second CTD transect following approximately the same trajectory of the first one, was conducted a week later on 21 March (Fig. 6b), 4 days after the end of the easterlies period. The hydrological structure of the water column had changed dramatically with respect to 14 March, showing a substantial shoaling of the isopycnals. A remarkably homogenous water mass with the hydrological properties of oAW and low SSC filled the upper 400 m of the water column inside the canyon, replacing the turbid, cold and freshened intrusion as well as the underlying water mass with WIW characteristics noticeable on 14 March.

4.4 Horizontal and downward particle fluxes at the south canyon flank

Time-series of temperature, current speed, SSC, horizontal and downward sediment flux at the two lines deployed on the southern canyon flank (SF1, SF2), together with significant wave height and river discharge in the study area are shown in Figs. 7 and 8, respectively.

4.4.1 Line SF1

At line SF1 located on the southern canyon wall at 260 m depth, horizontal and settling flux were low until 13 March, without any clear signal of the 8 March storm except for a timid increase of current speed that did not produce a significant sediment transport. During the two consecutive storms of 13–15 March, apparent downward mass fluxes increased to up to two orders of magnitude while downcanyon fluxes of suspended sediment increased by up to 4 orders of magnitude. The downward particle flux estimated from sediment traps was relatively stable around 125–150 $\text{g m}^{-2}\,\text{d}^{-1}$ during the main stormy period, and the horizontal flux peaked at a maximum 15 $\text{g m}^{-2}\,\text{s}^{-1}$ measured at 75 mab during the last storm (15 March). The cumulative sediment transport was almost 1.5 t m^{-2} at 75 mab and 0.85 t m^{-2} at 115 mab. Silt dominated the grain-size distribution of particles collected by the trap during all the deployment. Particles were coarsest, arriving to sand-size, during the period of highest horizontal and downward flux (Fig. 7).

4.4.2 Line SF2

The relative similarity of current speed, SSC and sediment flux at 75 and 115 mab that was patent at SF1 was even more marked at SF2, as it was the response in terms of increasing current speeds inside the canyon to increasing wave heights on the shelf (Fig. 8). In contrast to the canyon head line and SF1, the effects of the 8 March storm were noticeable at this station as an increase of both SSC and apparent settling flux during the same period. As it was the case at SF1, the main period of sediment transport corresponded to the stormy period of 12–15 March and preceded the peak of GoL rivers flooding. Current speeds were even higher at this site, reaching up to 90 cm s^{-1} during the peak of the 13 March storm. The strongest sediment transport pulse took place during the last storm on 15 March when the horizontal sediment flux reached almost 12 g m^{-2} s^{-1} at both monitored depths. The time-integrated estimated horizontal sediment transport at this site was between 0.8 and 0.9 t m^{-2} and remarkably similar at 75 and 115 mab. As in SF1, particle size and apparent downward mass flux at 40 mab was maximum during the main period of eastern storms and peaked at 217 g m^{-2} d^{-1} from 14 to 15 March (Fig. 8).

5 Discussion

Previous studies highlighted the prominent role of both DSWC and shelf storms in the offshore sediment transport in the western end of the GoL, particularly when these two physical phenomena occur intensely and in synergy (or within a same season or year) and with enough intensity, resuspending and advecting sediments towards the deep following a multi-step scheme (Bonnin et al., 2008; Ulses et al., 2008a; Palanques et al., 2006, 2008). In contrast with the precedent literature on shelf-to-basin sediment transport in the GoL, which has been mainly devoted to the impact of extreme events, the present work helps to gain insight on the response of the canyon to meteorological conditions representative of an average year without extreme events.

Along-canyon off-shelf transport is known to be greater during years of intense cascading (Canals et al, 2006; Puig et al., 2008; Palanques et al., 2012). Winter 2010–2011 was relatively warm and wet with weak formation of dense water in the GoL (Rumín-Caparrós et al., 2012). In fact, the time-series of horizontal and settling particle fluxes at the canyon head (Fig. 3) reflect the lack of extreme meteorological events during this winter and were relatively low when compared with previous years (Palanques et al., 2006; Ribó et al., 2011; Rumín-Caparrós et al., 2012).

Nonetheless, a sequence of 2 moderate eastern storms produced notable transport of sediments through the CCC, particularly along its southern flank, even though fluxes were weak at the canyon head.

5.1 Mechanisms and sources implied in the observed particle fluxes

Most of the sediment transport during the study took place within a short period (13–15 March) including two consecutive eastern storms. During the onset of the 12–13 March storm, the progressive downwelling associated to eastern winds was visible as warmer and less dense water was progressively pushed down to the bottom at 300 m depth (Fig. 5). Subsequently, a cold and turbid water mass occupied the canyon from 150–200 to 350 m depth. Most of the sediment transport calculated during this study was associated to that intrusion that was observed, mainly along the southern canyon wall from 13 to 15 March.

If considered alone, the low temperature of this water mass could lead to interpret it as dense water newly formed by convection over the shelf. But, contrary to our initial expectations, the abrupt decrease in water temperature observed inside the canyon during 13–16 March (Figs. 4, 5, 6) was not related to a tongue of cascading dense water, as evidenced by simultaneous measurements of water temperature and conductivity with CTD probes, that allowed a precise determination of the density anomaly of this water body (Figs. 5, 6 and 9). Its position in the T/S diagram (Figs. 10 and 11) and namely its density ($\sim 28.78\,\text{kg}\,\text{m}^{-3}$) do not qualify it to cascade down-canyon driven by negative buoyancy or even to form shallow WIW.

The turbid water mass observed during these dates inside the canyon was in fact lighter than the waters occupying the same depth stratum before and after the main period of eastern storms and very likely was pushed into the canyon below its equilibrium depth by storm-induced downwelling (Palanques et al., 2008; Ulses et al., 2008b). In that regard, it is noteworthy the apparent correlation (with a slight temporal decoupling

$\sim$10 h) of increases in significant wave height on the shelf and downcanyon current speeds (Figs. 4, 7, 8). We will thereafter refer to this water mass as “Coastal Waters”, a generic label for a water mass that we believe is strongly influenced by freshwater discharge and/or continental runoff, given its low salinity. The low temperature and low salinity of the water mass intruding the canyon during 13–15 March fits with a coastal origin, taking into account that both the temperature and salinity of the Rhône plume tend to be significantly lower than the surrounding waters, at least during winter (e.g. Omnes et al., 1996). Similar T/S hydrological signatures as the “coastal waters” described in this work (Figs. 10, 11) have been reported by Dufau-Julliand et al. (2004) over the inner GoL shelf and by Vargas-Yañez et al. (2012) in coastal areas under the influence of the other major western Mediterranean river, the Ebro. The surface and shelf/coastal origin of this water mass was also evidenced by its high oxygen content and particle load (Fig. 6). The coastal plume extended to a depth of $\sim$350 m, in the limit with an underlying water mass showing the hydrological signature of WIW (Fig. 11). This later water mass could have been formed earlier that winter on the shelf, possibly in December when maximum heat losses took place (Rumín-Caparrós et al., 2012) and the most acute temperature drop of the winter was recorded at the canyon head (Fig. 3) or more probably during a prolonged Tramontane period that preceded the CASCADE cruise (21 February to 3 March, see Fig. 3). Alternatively, WIW can also be formed offshore and then advected shoreward following the general circulation (Lacombe and Tchernia, 1972) and in fact WIW formation by winter mixing was observed offshore from the GoL in December 2010 and January 2011.

The eastern storms that hit the GoL from 12 March produced substantial precipitations in the Massif Central and particularly the Pyrenees watersheds where some rivers reached water discharge with return periods up to 5–15 yr (Bourrin et al., 2012). However, these important freshwater inputs did not seem to influence the water mass detected in the canyon by 13 March and labelled as “Coastal waters”, since river discharge was actually low just before and during the onset of that storm and only increased notably some days after. It follows then that the SE storm of 12–13 March only flushed the freshened coastal waters without the interplay of simultaneous flooding.

The same that has just been stated for the contribution of regional river discharge to the plume of coastal waters is also applicable to sediment budgets. It is unlikely that sediment inputs associated to these important freshwater discharges can justify the horizontal and downward mass flux increases observed from 13 to 15 March along the South CCC flank, because the maximum river discharge was peaking when horizontal and settling particle fluxes inside the canyon were already in decline. In fact, it has been shown in the past that most of the sediments delivered by GoL rivers remain close to the river mouth after floods and is only remobilized later when energetic conditions develop again (Guillén et al., 2006). An altimeter placed at the POEM site on the adjacent inner shelf documented a sharp change in depth (= 4 cm) just upon the passage of the 13 March storm (Bourrin et al., 2012), confirming that erosion of inner shelf sediments by storm waves, rather than river discharge, was the main source of sediments associated to the shelf water mass flowing along the coast and then plunging inside the canyon.

Water column stratification is another important parameter to take into account to investigate the intensity of offshelf transport episodes (Palanques et al., 2008). The storm of 13 March did not only erode shelf sediments and induced downwelling but primarily mixed the upper water column. As a consequence, the following storm (15 March) occurred under weaker stratification conditions, favouring the penetration to greater depths of the coastal waters. In fact, sediment transport at all depths and stations was maximal during the 15 March storm (Figs. 7, 8).

5.2 Horizontal sediment transport and settling particle fluxes in the CCC during March 2011

In previous studies addressing the transport associated to storm events in the GoL, priority was given to deploying sets of instruments near the seafloor, assuming that most of the sediment transport was relatively confined near the bottom or more relevant than at intermediate depths. The present results seem to challenge that notion. In fact, during the main period of eastern storms and the associated downwelling, sediment transport was remarkably homogeneous in a depth range of 150–350 m along the southern canyon flank, as suggested by horizontal sediment fluxes in the same order of magnitude at 75 and 115 mab above the seafloor at both mooring sites SF1 and SF2.

In order to estimate the total transport associated to the cold water intrusion, and since only punctual (turbidimeter deployment heights) sediment flux has been obtained at the mooring sites, we will rely on the CTD transect of 14 March, where more continuous and simultaneous measurements of SSC (Seapoint turbidimeter attached to the CTD probe) and current speed (ship-based ADCP) are available. Total transport has been estimated in parcels of 16 m height (the bin size of the ADCP) and length the average distance between consecutive CTD stations. The resulting area was multiplied by the along-canyon suspended sediment flux. Previously, SSC data was resampled to meet the vertical resolution of current speed measurements. Assuming that the thickness, turbidity and speed of the plume of shelf waters observed on 14 March (Fig. 6) was representative of the main downwelling period lasting about 3 days (13–15 March), a transport of 10^5 metric tons of sediment has been estimated as being transferred along the southern canyon flank within the turbid intrusion of coastal waters. This represents about 1 % of the average annual sediment load delivered by the Rhône River (Bourrin et al., 2006). These numbers fit with the punctual sediment flux estimated at 75 and 115 mab at SF1 and SF2 (0.8–$1.5\,\mathrm{t\,m^{-2}}$), considering the thickness and lateral extension of the turbid plume. Also, it is possible that we have underestimated the total sediment transport, given that the horizontal particle flux measured at SF1 and SF2 was still relatively low during the 14 March transect and peaked markedly a day later in coincidence with the last storm of the deployment period (Figs. 7, 8).

5.3 Transport routes during eastern storms

Previous studies suggested that during major episodes of offshore transport such as cascading and storm-induced downwelling, the main water flow tends to follow the coastline, affecting to some degree the CCC head but entering the canyon preferentially by the southern flank. This scheme was setup by comparing simultaneous observations from 750 m depth in the canyon axis and the canyon head at 300 m (Canals et al., 2006; Puig et al., 2008; DeGeest et al., 2008) and also by means of numerical models (Ulses et al., 2008b). However this point was not yet clearly demonstrated with direct observations on the southern canyon flank.

At the canyon head (CH), where a long-term station allows an interannual comparison, the mild meteorological context of winter 2011 is reflected in weak sediment fluxes. In particular, during the CASCADE cruise the downward mass flux estimated with a sediment trap at 40 mab was $< 10\,\mathrm{g\,m^{-2}\,d^{-1}}$, the horizontal particle flux always below $4\,\mathrm{g\,m^{-2}\,s^{-1}}$ and the cumulative transport did not surpass $0.6\,\mathrm{t\,m^{-2}}$. These values are inferior to those measured in previous winters and among the lowest measured at that station since it was incepted in autumn 2004 (Canals et al., 2006; Palanques et al., 2006; 2012; Ribó et al., 2011; Rumín-Caparrós et al., 2012).

These weak horizontal and settling fluxes measured in the canyon head in March 2011 strongly contrast with the intense transport observed in the southern canyon flank during the same period. Sediment transport at both 75 and 115 mab in the southern flank (both lines SF1 and SF2) was higher than near the bottom (5 mab) at the canyon head (CH). In particular, sediment transport at 75 mab in line SF1 ($1.5\,\mathrm{t\,m^{-2}}$) was almost three times the one calculated at the canyon head near the bottom ($0.6\,\mathrm{t\,m^{-2}}$), thus indicating preferential transport along the canyon flank.

Also, it is noteworthy that the first and weakest storm (8 March, $H_s = 3.3\,\mathrm{m}$) had no noticeable influence on particle fluxes at CH or SF1 (Figs. 4, 7), while it clearly impacted the deepest station SF2 (Fig. 8). This confirms the previously held idea that turbid plumes tend to contour the canyon rim flowing close to the coastline and enter it by its downstream side upon encountering the constrain of the Cap de Creus Peninsula. When stratification is weaker or more energetic conditions develop, the entire canyon is impacted.

Also sediment traps recorded apparent fluxes one order of magnitude higher in the southern canyon flank than at CH during the main period of eastern storms. Given the wide difference in sampling intervals between traps deployed in the south canyon flank (35 h) and in the canyon head (15 days), a better comparison can be achieved by integrating the mass flux data for the ensemble of the collecting period (4–19 March). The total settling flux thus estimated mounts to 51.2 $g\,m^{-2}\,d^{-1}$ and 55.4 $g\,m^{-2}\,d^{-1}$ at SF1 and SF2 respectively, whereas it amounts to an estimated value of only 8.5 $g\,m^{-2}\,d^{-1}$ in the canyon head for the same period. These numbers and comparisons must however be taken with caution because the strong oscillations experienced by the mooring lines during the periods of maximum flux (see Fig. 2 and Sect. 2.1.3) may have affected the collection efficiency of sediment traps (Gardner, 1985).

5.4 Exit routes of transient intermediate waters and implications for canyon morphology

As the dominant eastern wind field veered to northwesterlies on 16–17 March, the flow inside the canyon reversed and the isopycnals were pushed up (Figs. 4, 6b), indicating that the plume of turbid and cold water that entered the canyon during the storm returned to its equilibrium depth at 50 m depth and hence left the canyon confinement. This compensation of the isopycnals has been described as the reversal (relaxation) phase of downwelling events (Ulses et al., 2008b). Once freed from topographic control, this water mass was likely forced to flow with the mean SW circulation imposed by the Northern Current.

It has been stated that, during severe winters when shelf waters attain higher density following strong cooling and evaporation and the upper water column is more homogeneous, DSWC flows obliquely along the southern flank of the canyon producing on its way furrow fields which extends down to 1500 m deep (Canals et al., 2006; Lastras et al., 2007; Puig et al., 2008). On the other hand, the possible influence of storm-induced downwelling and associated current bursts around the shelf-break depth on the present-day shaping of the margin are still understudied. Figure 12 schematizes the main contemporary processes of seafloor shaping in the CCC seabed, including the formation of furrows in the deep canyon axis by the erosive action of deep DSWC (blue arrow in Fig. 12). Shallower cascading or the storm-induced downwelling process described in this work would rather follow the paths marked by orange arrows in Fig. 12. Polar plots of currents from the topmost and bottommost ADCP cells with valid data have also been plotted in Fig. 12. Currents closer to the seafloor were weaker and more scattered than topmost currents at the level of the canyon rim. The later are clearly directed towards the scars visible in the canyon wall. The recurrence of E-SE storm events in the Gulf of Lion (with at least one significant storm each year) suggest, on the long-term, a causative relationship between the episodic sediment transport capacity of the strong storm-induced currents and these erosive features at the canyon rim.

Eastern storms can transport silt- and sand-sized particles in suspension (Figs. 7, 8), able to abrade the canyon flank. The erosional results of the processes described here eventually overlap by those caused by shallow dense shelf water cascading following the same gross direction.

6 Conclusions

We have documented a remarkable episode of sediment transport along the southern flank of the Cap de Creus Canyon during a series of moderate eastern storms and in the context of a mild and wet winter 2010–2011.

Most of the along-canyon sediment transport during the monitored period (3–22 March 2011) took place during a relatively short episode (13–15 March) of dominant eastern winds comprising two consecutive storms with H_s in the range 4–4.6 m. During this period, a tongue of cold freshened and turbid water of shelf/coastal origin subdued into the canyon along its southern flank to depths up to 350 m. The intruding water was less dense than ambient waters, being pushed below its equilibrium depth by storm-induced downwelling. Sediment transport along the canyon flank was remarkably well distributed in a range of 200 m above the bottom without near-bottom constriction.

10^5 t of sediments have been estimated as being transported into the canyon within the downwelled coastal plume during the 3-day stormy period.

Regional rivers flooded after the main period of eastern storms and hence were not the main contributors to suspended sediments inside the canyon during the downwelling phase. Instead, erosion of inner shelf sediments by the action of storm waves was likely the primary source of sediments feeding the suspended particle pool of the coastal water plume intruding the canyon.

This study highlights that Cap de Creus Canyon, and particularly its southern flank, is a very significant channel for across-isobath sediment transport also during mild meteorological forcing conditions in the absence of dense shelf water cascading.

Erosional marks in the southern canyon flank, carved in an orientation coherent with the strongest water flows measured during eastern storms, indicate that they can be at least partly caused by repeated downwelling and evacuation of intermediate water bodies during the frequent and short-lived eastern storms characteristic of the study area.

A bottom line to these observations is that, in the study area, concomitant and accurate measurements of water conductivity must complement near-bottom water temperature monitoring programs in order to correctly interpret drops of water temperature that otherwise could be attributed solely to dense water cascading.

Acknowledgements. We are grateful to the crew and officials of R/V *l'Atalante* and to all the scientific and technical staff involved in the CASCADE cruise for their support during sea operations.

This work was funded by the HERMIONE Project (FP7-ENV-2008-1-226354) under the European Commission's Seventh Framework Programme, the French Program MERMEX under the

MISTRALS framework, the GRACCIE-CONSOLIDER project (CSD2007-00067) and the Spanish project DOS MARES (CTM2010-21810-C03-01). University of Barcelona researchers benefited from grant 2009 SGR 1305 by Generalitat de Catalunya to excellence research groups. L. Houpert acknowledges the support of the Direction Générale de l'Armement (supervisor: Elisabeth Gibert-Brunet). J. Martín was funded through a JAE-DOC contract within the Program "Junta para la Ampliación de Estudios", granted by Consejo Superior de Investigaciones Scientifics (Spain) and co-financed by the European Social Fund.

References

Allen, S. E. and Durrieu de Madron, X.: A review of the role of submarine canyons in deep-ocean exchange with the shelf, Ocean Sci., 5, 607–620, doi:10.5194/os-5-607-2009, 2009.

Bonnin, J., Heussner, S., Calafat, A., Fabres, J., Palanques, A., Durrieu de Madron, X., Canals, M., Puig, P., Avril, J., and Delsaut, N.: Comparison of horizontal and downward particle fluxes across canyons of the Gulf of Lions (NW Mediterranean): Meteorological and hydro dynamical forcing, Cont. Shelf Res., 28, 1957–1970, 2008.

Bougis, P. and Ruivo, M.: Sur une descente des eaux superficielles en profondeur (cascading) dans le sud du Golfe du Lion, Bulletin d'Information du Comité Central d'Océanographie et d'Etude des Côtes, 6, 147–154, 1954.

Bourrin, F., Durrieu de Madron, X., and Ludwig, W.: Contribution to the study of coastal rivers and associated prodeltas to sediment supply in the Gulf of Lions, Life Environ., 56, 307–314, 2006.

Bourrin, F., Durrieu de Madron, X., Heussner, S., and Estournel, C.: Impact of winter dense water formation on shelf sediment erosion (evidence from the Gulf of Lions, NW Mediterranean), Cont. Shelf Res., 28, 1984–1999, 2008.

Bourrin, F., Durrieu de Madron, X., Beguery, L., Martín, J., and Houpert, L.: Sediment resuspension and fluxes estimated from glider during a typical winter storm in the Gulf of Lions, NW Mediterranean, in preparation, 2012.

Buscail, R. and Germain, C.: Present-day organic matter sedimentation on the NW Mediterranean margin: Importance of off-shelf export, Limnol. Oceanogr., 42, 217–229, 1997.

Canals, M., Puig, P., Durrieu de Madron, X., Heussner, S., Palanques, A., and Fabres, J.: Flushing submarine canyons, Nature, 444, 354–357, 2006.

DeGeest, A. L., Mullenbach, B. L., Puig, P., Nittrouer, C. A., Drexler, T. M., Durrieu de Madron, X., and Orange, D. L.: Sediment accumulation in the western Gulf of Lions, France: The role of Cap de Creus Canyon in linking shelf and slope sediment dispersal systems, Cont. Shelf Res., 28, 2031–2047, 2008.

Dewey, R. K.: Mooring Design & Dynamics – a Matlab® package for designing and analyzing oceanographic moorings, Mar. Models, 1, 103–157, 1999.

DREAL: http://www.languedoc-roussillon.developpement-durable.gouv.fr/IMG/pdf/DREAL_LR-rapport_coup_de_mer_12-16_mars_2011_cle5d39f7.pdf., 2011.

Drexler, T. M. and Nittrouer, C. A.: Stratigraphic signatures due to flood deposition near the Rhône River: Gulf of Lions, northwest Mediterranean Sea, Cont. Shelf Res., 28, 1877–1894, 2008.

Dufau-Julliand, C., Marsaleix, P., Petrenko, A., and Dekeyser, I.: Three-dimensional modeling of the Gulf of Lion's hydrodynamics (north-west Mediterranean) during January 1999 (MOOGLI3 Experiment) and late winter 1999: Western Mediterranean Intermediate Water's (WIW's) formation and its cascading over the shelf break, J. Geophys. Res., 109, C11002, doi:10.1029/2003JC002019, 2004.

Durrieu de Madron, X., Zervakis, V., Theocharis, A., and Georgopoulos, D.: Comments on "Cascades of dense water around the world ocean", Prog. Oceanogr., 64, 83–90, 2005.

Durrieu de Madron, X., Wiberg, P. L., and Puig, P.: Sediment dynamics in the Gulf of Lions: The impact of extreme events, Cont. Shelf Res., 28, 1867–1876, 2008.

Ferré, B., Guizien, K., Durrieu de Madron, X., Palanques, A., Guillén, J., and Grémare, A.: Fine sediment dynamics study during a winter storm in the Gulf of Lion shelf (NW Mediterranean), Cont. Shelf Res., 25, 2410–2427, 2005.

Firing, E. and Hummon, J. M.: Ship-mounted Acoustic Doppler Current Profilers, in: The GO-SHIP Repeat Hydrography Manual: A Collection of Expert Reports and Guidelines, edited by: Hood, E. M., Sabine,C. L., and Sloyan, B. M., IOCCP Report Number 14, ICPO Publication Series Number 134, available at: http://www.go-ship.org/HydroMan.html, 2010.

Firing, E., Ranada, J., and Caldwell, P.: Processing ADCP data with the CODAS Software System Version 3.1., User manual, Joint Institute for Marine and Atmospheric Research, University of Hawaii, USA, available at http://epic.awi.de/29904/1/Fir1995b.pdf, 1995.

Flexas, M. M., Durrieu de Madron, X., Garcia, M. A., Canals, M., and Arnau, P. : Flow variability in the Gulf of Lions during the MATER HFF experiment (March–May 1997), J. Marine Syst., 33–34, 197–214, 2008.

Fofonoff, N. P. and Millard, R. C.: Algorithms for computation of fundamental properties of seawater, UNESCO Tech. Papers Mar. Sci., 44, 1–53, 1983.

Gardner, W. F.: The effect of tilt on sediment trap efficiency, Deep-Sea Res., 32, 349–361, 1985.

Guillén, J., Palanques, A., Puig, P., Durrieu de Madron X., and Nyffeler, F.: Field calibration of optical sensors for measuring suspended sediment concentration in the western Mediterranean, Sci. Mar., 64, 427–435, 2000.

Guillén, J., Bourrin, F., Palanques, A., Durrieu de Madron, X., Puig, P., and Buscail, R.: Sediment dynamics during 'wet' and 'dry' storm events on the Têt inner shelf (SW Gulf of Lions), Mar. Geol., 234, 129–142, 2006.

Harris, P. T. and Whiteway, T.: Global distribution of large submarine canyons: Geomorphic differences between active and passive continental margins, Mar. Geol., 285, 69–86, 2011.

Heussner, S., Ratti, C., and Carbonne, J.: The PPS 3 time-series sediment trap and the trap sample processing techniques used during the ECOMARGE experiment, Cont. Shelf. Res., 10, 943–958, 1990.

Heussner, S., Calafat, A., and Palanques, A.: Quantitative and qualitative features of particle fluxes in the North Balearic basin, edited by: Canals, M., Casamor, J. L., Cacho, I., Calafat, A. M., and Monaco, A., Euromarge-NB final report, MAST II program, EU, IIIB, RGMG-University of Barcelona, Barcelona, 43–66, 1996.

Heussner, S., Durrieu de Madron, X., Calafat, A., Canals, M., Carbonne, J., Delsaut, N., and Saragoni, G.: Spatial and temporal variability of downward particle fluxes on a continental slope: Lessons from an 8-yr experiment in the Gulf of Lions (NW Mediterranean), Mar. Geol., 234, 63–92, 2006.

Hickey, B. M.: The response of a steep-sided, narrow canyon to time-variable wind forcing, J. Phys. Oceanogr., 27, 697–728, 1997.

Huthnance, J. M.: Circulation, exchange and water masses at the ocean margin: the role of physical processes at the shelf edge, Prog. Oceanogr., 35, 353–431, 1995.

Jahnke, R. A., Reimers, C. E., and Craven, D. B.: Intensification of recycling of organic matter at the sea floor near ocean margins, Nature, 348, 50–54, 1990.

Lacombe, H. and Tchernia, P.: Le problème de la formation des eaux marines profondes. Déroulement du phénomène en Méditerranée Nord-Occidentale par hiver très froid (Janvier–Mars 1963), Ann. Inst. Océanogr., 48, 1–112, 1972.

Lapouyade, A. and Durrieu de Madron, X.: Seasonal variability of the advective transport of particulate matter and organic carbon in the Gulf of Lion (NW Mediterranean), Oceanol. Acta, 24, 295–312, 2001.

Lastras, G., Canals, M., Urgeles, R., Amblàs, D., Ivanov, M., Droz, L., Dennielou, B., Fabrés, J., Schoolmeester, T., Akhmetzhanov, A., Orange, D., and García-García, A.: A walk down the Cap de Creus canyon, northwestern Mediterranean Sea: Recent processes inferred from morphology and sediment bedforms, Mar. Geol., 246, 176–192, 2007.

Martín, J., Palanques, A., and Puig, P.: Near-bottom horizontal transfer of particulate matter in the Palamós submarine canyon (NW Mediterranean), J. Mar. Res., 65, 193–218, 2007.

Martín, J., Palanques, A., Vitorino, J., Oliveira, A., and de Stigter, H.: Near-bottom downward flux of particulate matter in the Nazaré submarine canyon during normal and stormy conditions, Deep-Sea Res. Part II, 58, 2388–2400, 2011.

Millot, C.: Circulation in the Western Mediterranean Sea, J. Mar. Syst., 20, 423–442, 1999.

Monaco, A., Courp, T., Heussner, S., Carbonne, J., Fowler, S. W., and Deniaux, B.: Seasonality and composition of particulate fluxes during ECOMARGE-I western Gulf of Lions, Cont. Shelf Res., 9–11, 959–987, 1990.

Omnes, P., Slavyk, G., Garcia, N., and Bonin, P.: Evidence of denitrification and nitrate ammonification in the River Rhône plume (northwestern Mediterranean Sea), Mar. Ecol.-Prog. Ser., 141, 275–281, 1996.

Palanques, A., Durrieu de Madron, X., Puig, P., Fabres, J., Guillén, J., Calafat, A., Canals, M., Heussner, S., and Bonnin, J.: Suspended sediment fluxes and transport processes in the Gulf of Lions submarine canyons, The role of storms and dense water cascading, Mar. Geol., 234, 43–61, 2006.

Palanques, A., Guillén, J., Puig, P., and Durrieu de Madron, X.: Storm-driven shelf-to-canyon suspended sediment transport at the southwestern end of the Gulf of Lions, Cont. Shelf Res. 28, 1947–1956, 2008.

Palanques, A., Puig, P., Guillén, J., Durrieu de Madron, X., Latasa, M., Scharek, R., and Martin, J.: Effects of storm events on the shelf-to-basin sediment transport in the southwestern end of the Gulf of Lions (Northwestern Mediterranean), Nat. Hazards Earth Syst. Sci., 11, 843–850, doi:10.5194/nhess-11-843-2011, 2011.

Palanques, A., Puig, P., Durrieu de Madron, X., Sánchez-Vidal, A., Pascual, C., Martín, J., Calafat, A., Heussner, S., and Canals, M.: Deep canyon and slope sediment resuspension and transport in the western Gulf of Lions during the 2006 intense cascading and open sea convection period, Prog. Oceanogr., 106, 1–15, 2012.

Pfannkuche, O.: Benthic response to the sedimentation of particulate organic matter at the BIOTRANS station, 47 N, 20 W, Deep-Sea Res. Part II, 40, 135–149, 1993.

Puig, P., Palanques, A., Sanchez-Cabeza, J. A., and Masqué, P.: Heavy metals in particulate matter and sediments in the southern Barcelona sedimentation system (North-western Mediterranean), Mar. Chem., 63, 311–329, 1999.

Puig, P., Palanques, A., Guillén, J., and El Khatab, M.: Role of internal waves in the generation of nepheloid layers on the northwestern Alboran slope: Implications for continental margin shaping, J. Geophys. Res., 109, C09011, doi:10.1029/2004JC002394, 2004.

Puig, P., Palanques, A., Orange, D. L., Lastras, G., and Canals, M.: Dense shelf water cascades and sedimentary furrow formation in the Cap de Creus Canyon, northwestern Mediterranean Sea, Cont. Shelf Res., 28, 2017–2030, 2008.

Ribó, M., Puig, P., Palanques, A., and Lo Iacono, C.: Dense shelf water cascades in the Cap de Creus and Palamós submarine canyons during winters 2007 and 2008, Mar. Geol., 284, 175–188, 2011.

Rumín-Caparrós, A., Sanchez-Vidal, A., Calafat, A. M., Canals, M., Puig, P., Martín, J., and Pedrosa-Pàmies, R.: External forcings, oceanographic processes and particle flux dynamics of Cap de Creus submarine canyon, NW Mediterranean Sea, Biogeosciences Discuss., accepted, 2012.

Salat, J. and Cruzado, A.: Masses d'eau dans la Méditerranée Occidentale: Mer Catalane et eaux adjacentes, Rapp. Comm. int. Mer Médit., 27, 201–209, 1981.

Ulses, C., Estournel, C., Durrieu de Madron, X., and Palanques, A.: Suspended sediment transport in the Gulf of Lions (NW Mediterranean): impact of extreme storms and floods, Cont. Shelf Res. 28, 2048–2070, 2008a.

Ulses, C., Estournel, C., Bonnin, J., Durrieu de Madron, X., and Marsaleix, P.: Impact of storms and dense water cascading on shelf-slope exchanges in the Gulf of Lion (NW Mediterranean), J. Geophys. Res., 113, C02010, doi:10.1029/2006JC003795, 2008b.

Vargas-Yáñez, M., Zunino, P., Schroeder, K., López-Jurado, J. L., Plaza, F., Serra, M., Castro, C., García-Martínez, M. C., Moya, F., and Salat, J.: Extreme Western Intermediate Water formation in winter 2010, J. Mar. Syst., 105–108, 52–59, 2012.

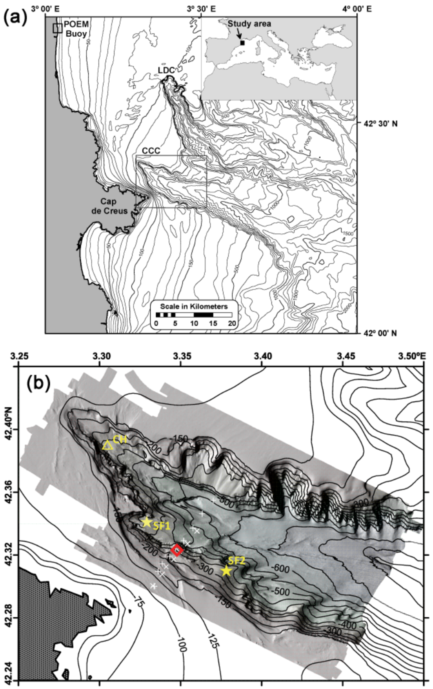

Fig. 1. (a) Bathymetric chart of the western Gulf of Lions showing the main submarine canyons in this area, the Lacaze-Duthiers (LDC) and Cap de Creus Canyon (CCC). The position of the POEM coastal site is also shown; **(b)** multibeam bathymetry of the CCC provided by Fugro Survey Ltd. and AOA Geophysics Inc. Stars mark the location of two temporary instrumented lines (SF1 and SF2) maintained in the southern canyon flank from 3 to 21 March 2011. The triangle marks the location of a long-term mooring line in the canyon head (CH). The position of a high resolution CTD station "CX" (11–14 March) is marked with a red diamond. White crosses represent CTD casts positions during two cross-canyon hydrological transects conducted on 14 and 21 March, the longest one corresponding to 14 March.

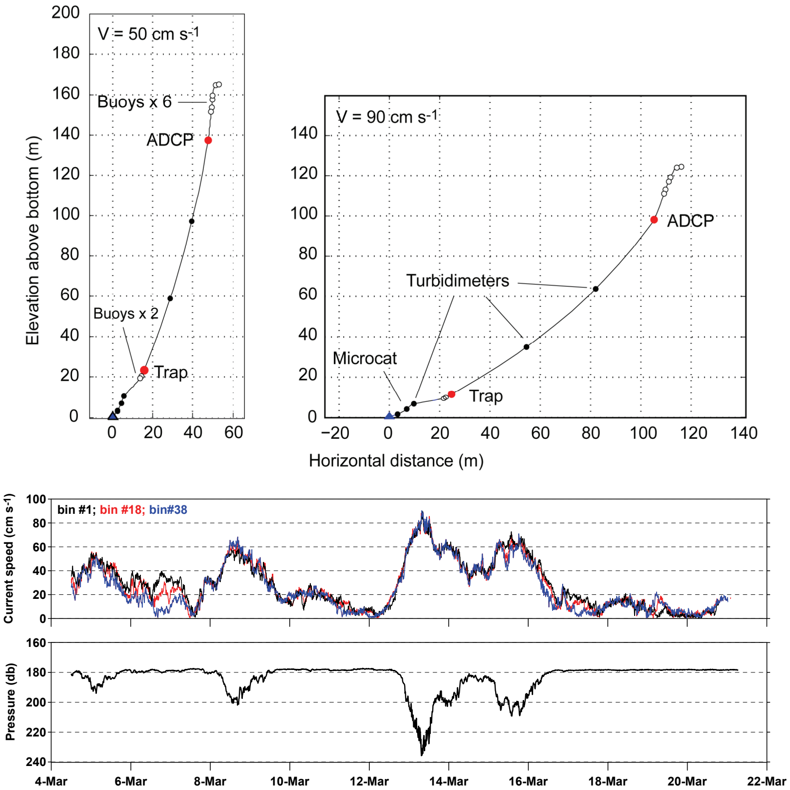

Fig. 2. Top: mooring dynamics as calculated by the Mooring Design and Dynamics Software under two selected current speeds; bottom: pressure and current speeds measured by an ADCP attached 160 m above the bottom to the temporary mooring line (SF2) that experienced the strongest currents. Current speeds correspond to three selected ADCP bins: the topmost bin and the two more critical bins corresponding to the position of Seapoint turbidimeters attached to the lines.

Title Page
Abstract | Introduction
Conclusions | References
Tables | Figures
◀I | ▶I
◀ | ▶
Back | Close
Full Screen / Esc
Printer-friendly Version
Interactive Discussion

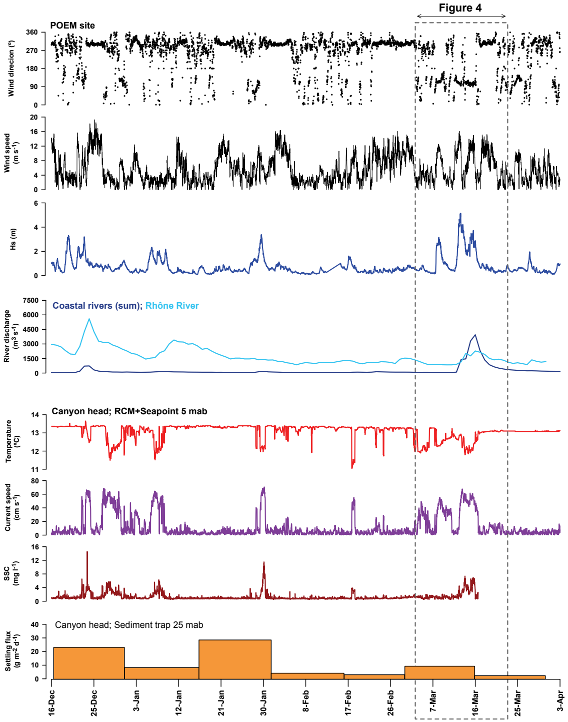

Fig. 3. General meteorological, hydrological and oceanographical setting in the study area, and hydrodynamic and particle flux response at the semi-permanent mooring line installed at the Cap de Creus Canyon head during winter 2010–2011. From top to bottom: wind speed, wind direction and significant wave height recorded at the POEM site (see Fig. 1a for location); mean daily water discharge of the Rhône River and the sum of coastal rivers opening to the Gulf of Lion; near-bottom water temperature, current speed, suspended sediment concentration and downward mass flux at the canyon head (300 m water depth). The dotted square marks the dates of the CASCADE cruise.

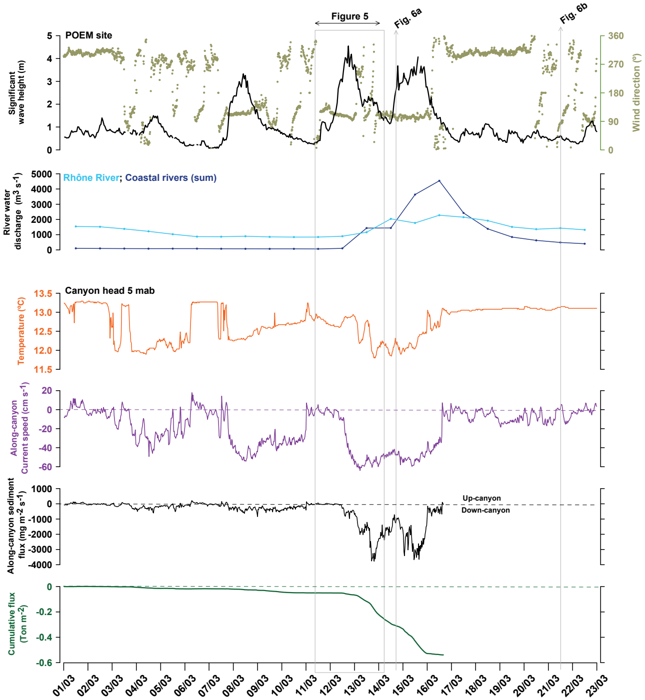

Fig. 4. Meteorological, hydrological and hydrodynamic context in the study area during the CASCADE cruise. From top to bottom: wind direction and significant wave height measured at the POEM coastal site; mean daily water discharge of the Rhône River and the sum of coastal rivers opening to the Gulf of Lion; near-bottom water temperature, along-canyon (130° rotated) current speed, sediment flux and cumulative sediment transport (positive values are offshore; negative onshore) at the canyon head. The dotted square marks the dates of a 3-day fixed CTD station (see the text and Figs. 5, 6). Vertical dotted lines correspond to two across-canyon CTD transects conducted before and after the main stormy period.

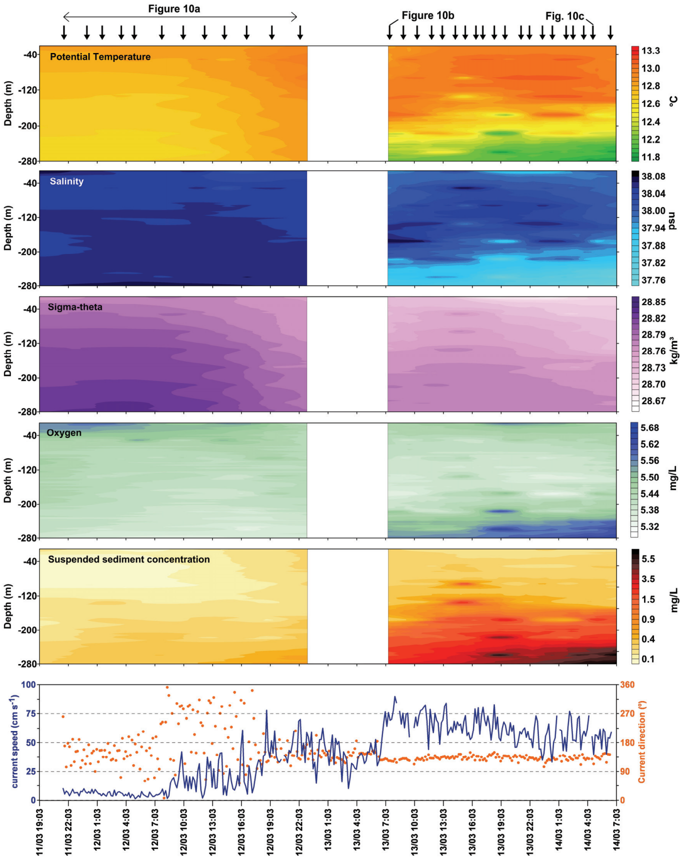

Fig. 5. Distribution of water column properties during the high-resolution temporal sampling at station CX in the Cap de Creus Canyon (see Fig. 1b for location). Arrows indicate the temporal distribution of CTD casts used to create the interpolated contours. Current speed and direction at 210 m depth measured by an ADCP installed on the ship hull are also shown.

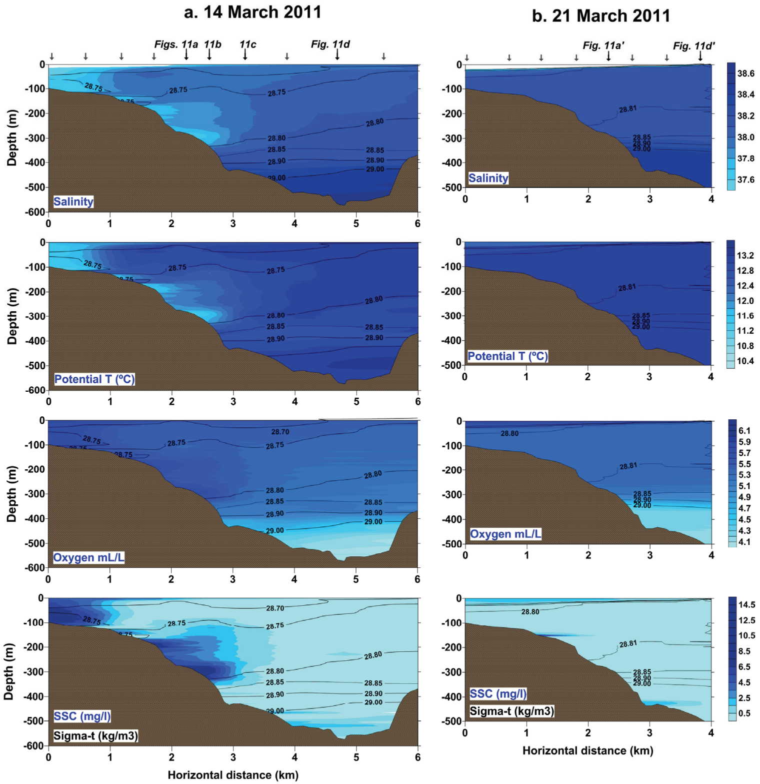

Fig. 6. Distribution of water column properties in the Cap de Creus Canyon during two across-canyon (= orthogonal to the canyon axis) CTD transects conducted on 14 and 21 March 2011 (left and right panels respectively). From top to bottom: water salinity, potential temperature, oxygen and suspended sediment concentration; isolines of water density anomaly are overlaid on all these contours. Top arrows mark the temporal distribution of CTD casts used to create the contours.

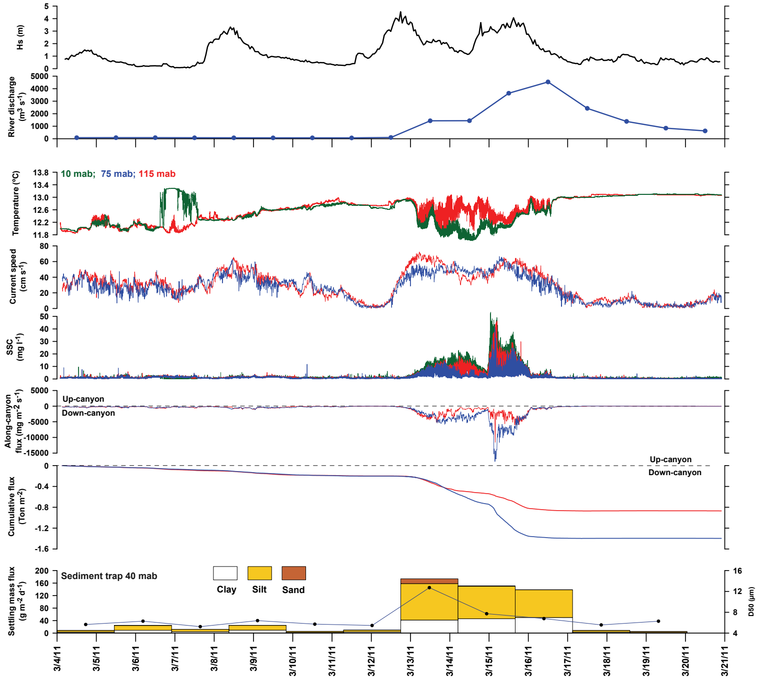

Fig. 7. Time-series of water and sediment fluxes in the Cap de Creus South canyon flank (mooring SF1, see Fig. 1b for location). From top to bottom: significant wave height measured at the POEM coastal site; total river discharge from coastal rivers opening to the Gulf of Lion (i.e. excluding the Rhône); in situ water temperature (measured by 3 Seapoint Aqualoggers), current speed measured by the ADCP at Seapoint depths, suspended sediment concentration (Seapoint); along-canyon sediment flux (negative values down-canyon); cumulative transport calculated from the precedent flux; downward mass flux measured by a sediment trap. Trap fluxes are divided in three components according to the major grain-size classes; the median of the grain-size distribution ($d50$) in sediment trap samples is also shown.

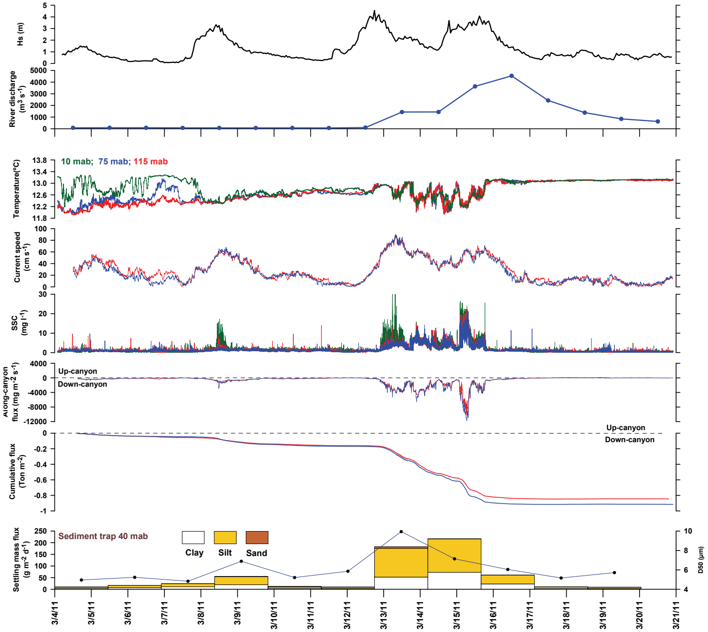

Fig. 8. Time-series of water and sediment fluxes in the Cap de Creus south canyon wall (mooring SF2, see Fig. 1b for location). From top to bottom: Significant wave height measured at the POEM site; total river discharge from coastal rivers opening to the Gulf of Lions (i.e. excluding the Rhône); in situ water temperature (measured by 3 Seapoint Aqualoggers), current speed measured by the ADCP at Seapoint depths, suspended sediment concentration (Seapoint), sediment flux rotated to meet the main canyon axis (negative values are down-canyon); cumulative transport calculated from the precedent flux; downward particle flux estimated from a sediment trap at 40 mab in the same mooring line. Trap fluxes are itemized in three major grain-size classes (clay, silt, sand), the median of the grain-size distribution ($d50$) is also shown.

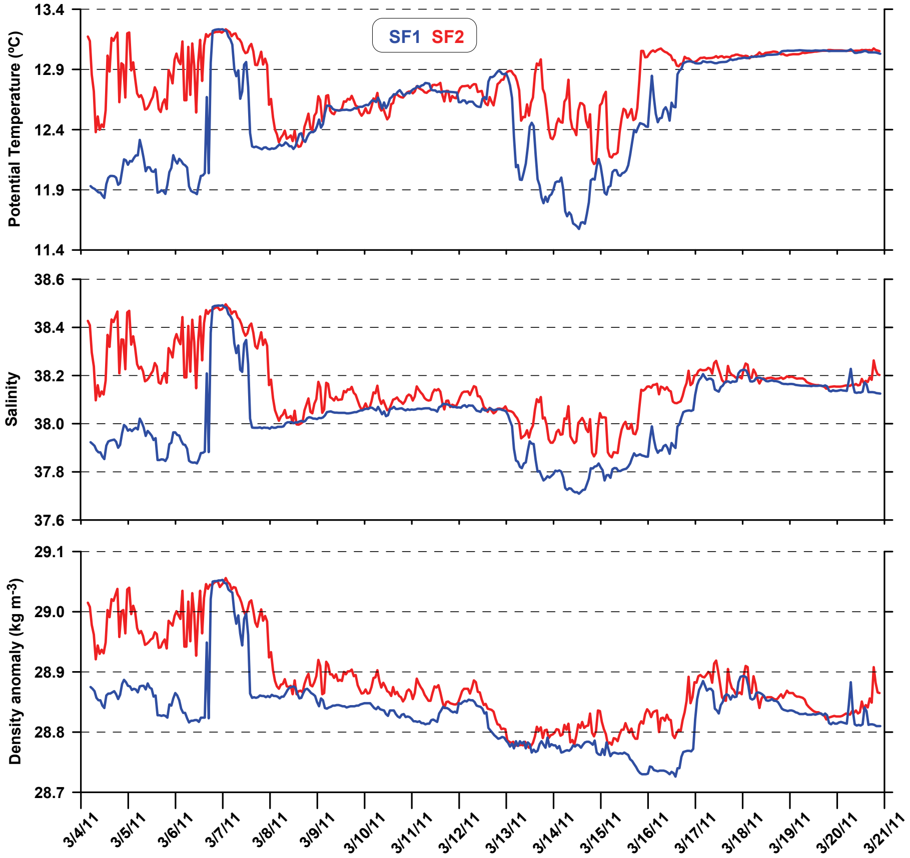

Fig. 9. Time series of potential temperature, salinity and density anomaly measured with a SBE 37-SMP probe attached 8 mab in the two mooring lines deployed on the southern CCC flank.

Title Page
Abstract | Introduction
Conclusions | References
Tables | Figures
◀| | |▶
◀ | ▶
Back | Close
Full Screen / Esc
Printer-friendly Version
Interactive Discussion

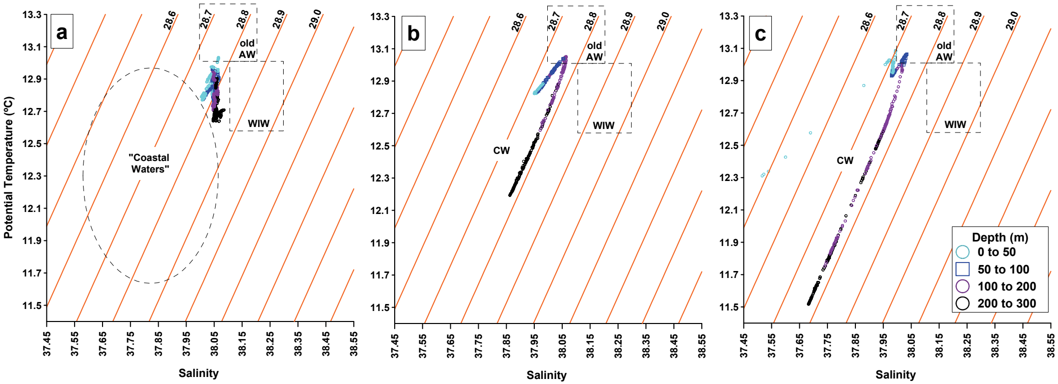

Fig. 10. *T*/*S* diagrams from selected CTD profiles conducted at the CX station in the Cap de Creus Canyon (see the text and Fig. 5 for details).

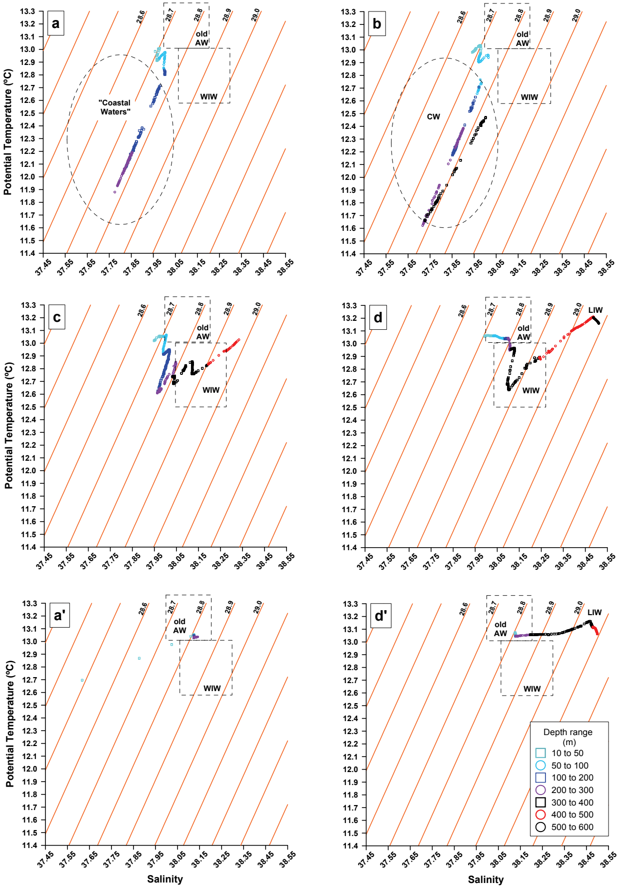

Fig. 11. *T*/*S* diagrams from selected vertical profiles (see Fig. 6 for positions) conducted during two CTD transects across Cap de Creus Canyon on 14 March **(a–d)** and 21 March (**a**′ and **d**′) 2011.

Title Page
Abstract | Introduction
Conclusions | References
Tables | Figures
I◀ | ▶I
◀ | ▶
Back | Close
Full Screen / Esc

Printer-friendly Version

Interactive Discussion

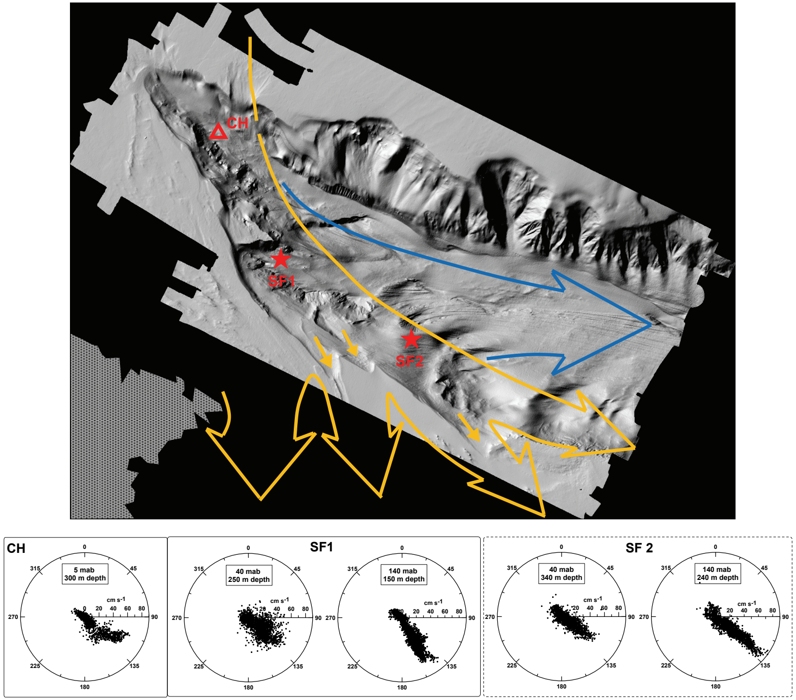

Fig. 12. Top: multibeam bathymetric map of the CCC, showing the main path of deep dense shelf water cascading (blue arrow) following the sedimentary furrows field, and the suggested path and exit routes for intermediate storm-downwelled shelf waters, hugging the southern canyon flank and causing scars on the canyon rims on the exit routes. Bottom: polar plots obtained from the canyon head station (CH, 5 mab) and the topmost (140 mab) and bottommost (50 mab) usable ADCP cells at the two mooring sites along the southern CCC flank are also shown. The blue arrow schematize the trajectory of deep cascading over a furrow field (see Puig et al., 2008) and orange lines the proposed routes for intermediate waters, originated whether by shallow cascading or storm-induced downwelling.